Phreatomagmatic eruptions on the Ontong Java Plateau: chemical and isotopic relationship to Ontong Java Plateau basalts

ROSALIND V. WHITE[1], PATERNO R. CASTILLO[2], CLIVE R. NEAL[3], J. GODFREY FITTON[4] & MARGUERITE GODARD[5]

[1]*Department of Geology, University of Leicester, University Road, Leicester LE1 7RH, UK (e-mail: rvw1@le.ac.uk)*

[2]*Geosciences Research Division, Scripps Institution of Oceanography, University of California, San Diego, La Jolla, CA 92093-0212, USA*

[3]*Department of Civil Engineering and Geological Sciences, University of Notre Dame, 156 Fitzpatrick Hall, Notre Dame, IN 46556, USA*

[4]*School of GeoSciences, University of Edinburgh, Grant Institute, West Mains Road, Edinburgh EH9 3JW, UK*

[5]*Laboratoire de Tectonophysique – CNRS UMR 5568, Case 49, Institut des Sciences de la Terre, de l'Eau et de l'Espace de Montpellier, Université de Montpellier II, Place Eugéne Bataillon, F-34095 Montpellier Cedex 5, France*

Abstract: The compositions of glass clasts in volcaniclastic rocks recovered from drilling at Site 1184 on the eastern salient of the Ontong Java Plateau (OJP) are investigated using microbeam analytical methods for major, minor and trace elements. These data are compared with whole-rock elemental and isotopic data for bulk tuff samples, and with data from basalts on the high plateau of the OJP. Three subunits of Hole 1184A contain blocky glass clasts, thought to represent the juvenile magmatic component of the phreatomagmatic eruptions that generated the volcaniclastic rocks. The glass clasts have unaltered centres, and are all basaltic low-K tholeiites, with flat chondrite-normalized rare earth element (REE) patterns. Their elemental compositions are very similar to the Kwaimbaita-type and Kroenke-type basalts sampled on the high plateau. Each subunit has a distinct glass composition and there is no intermixing of glass compositions between subunits, indicating that each subunit is the result of one eruptive phase, and that the volcaniclastic sequence has not experienced reworking. The relative heterogeneity preserved at Site 1184 contrasts with the uniformity of compositions recovered from individual sites on the high plateau, and suggests that the eastern salient of the OJP had a different type of magma plumbing system. Our data support the hypothesis that the voluminous subaerially erupted volcaniclastic rocks at Site 1184 belong to the same magmatic event as the construction of the main Ontong Java Plateau. Thus, the OJP would have been responsible for volatile fluxes into the atmosphere in addition to chemical fluxes into the oceans, and these factors may have influenced the contemporaneous oceanic anoxic event.

The Ontong Java Plateau (OJP), located in the equatorial western Pacific Ocean, is the world's largest oceanic plateau. Covering an area of 2.0×10^6 km^2, or eight times that of the UK, the OJP has an average crustal thickness of 30–35 km (Gladczenko *et al.* 1997; Richardson *et al.* 2000), and, in terms of volume, represents the largest documented igneous event on Earth. An enigmatic characteristic of the OJP is the fact that, despite its great thickness, it does not appear to have experienced sufficient uplift during magmatism to yield widespread subaerially erupted lavas. This is a paradox, as the size and extent of the OJP has led to widespread support for a large and vigorous mantle plume head being responsible for the magmatism (e.g. Richards *et al.* 1991; Saunders *et al.* 1992), in which case considerable uplift might be expected during volcanism. The observation that significant uplift seemingly did not occur suggests either that our models of mantle plume dynamics and/or oceanic plateau subsidence require modification, or even that alternative models for OJP formation should be re-examined. Neal *et al.* (1997) concluded that the impingement of the OJP plume head was insufficient to raise the high plateau above sea level, and the density of a hidden cumulate layer

From: FITTON, J. G., MAHONEY, J. J., WALLACE, P. J. & SAUNDERS, A. D. (eds) 2004. *Origin and Evolution of the Ontong Java Plateau*. Geological Society, London, Special Publications, **229**, 307–323. 0305-8719/$15.00

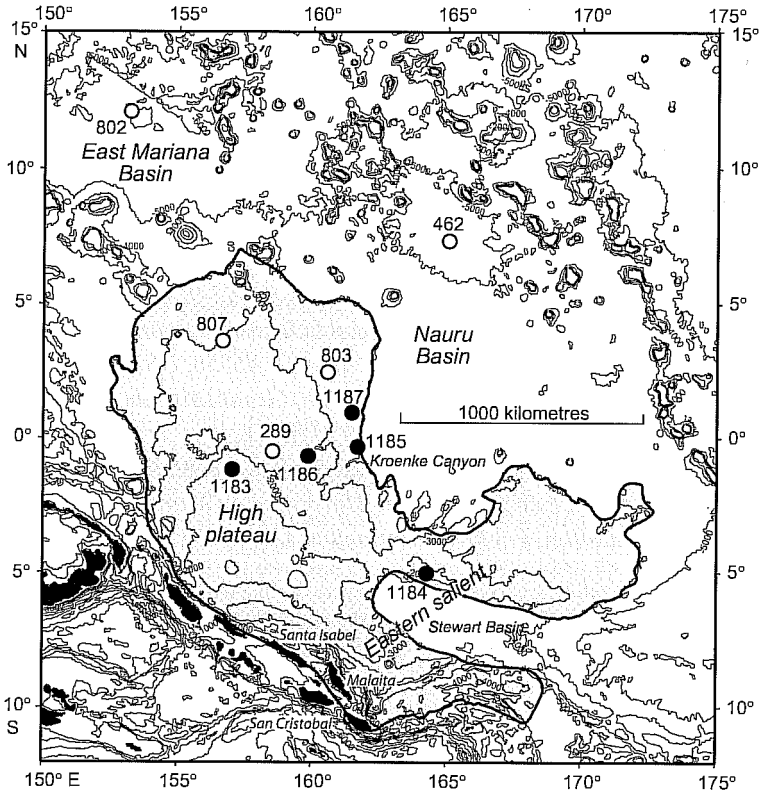

Fig. 1. Predicted bathymetry (after Smith & Sandwell 1997) of the OJP and surrounding areas showing the location of DSDP and ODP basement drill sites. The Ontong Java Plateau is shaded.

(complementary to the fractionated basalts) was sufficient to temper subsidence of the OJP such that it still stands above the surrounding ocean floor. Indeed, it is apparent that, at least along the northern and eastern margins of the OJP, the adjoining abyssal seafloor has subsided relative to the plateau (Kroenke 1972; Kroenke *et al.* 1986; Hagen *et al.* 1993).

Prior to Autumn 2000 and drilling of the OJP during Leg 192 of the Ocean Drilling Program, the volcanic basement of the plateau had been sampled at only three drill sites (DSDP Site 289 and ODP Sites 803 and 807) with limited penetration at each site (Andrews *et al.* 1975; Kroenke *et al.* 1991). This information was supplemented by studies of uplifted portions of the plateau in the Solomon Islands (e.g. Babbs 1997; Petterson *et al.* 1999; Birkhold 2000). One of the primary objectives of Leg 192 was to determine the environment and style of eruption at five widely separated sites in previously unsampled areas across the plateau (Fig. 1). In particular, a site at the current topographic high point of the plateau (Site 1183) was considered the location most likely to yield subaerial volcanic rocks. However, all of the basement sites sampled on the 'high plateau' are characterized by the presence of pillow basalts, with some massive flows and minor sedimentary interbeds. In fact, the basalt flows recovered from Site 1183 were very similar to the deep-water eruptives sampled on Malaita, Solomon Islands (Babbs 1997; Petterson *et al.* 1999; Tejada *et al.* 2002). This suggests that Ontong Java high plateau volcanism was confined largely to the submarine realm. In contrast, drilling at Site 1184, located on the previously unsampled 'eastern salient' of the OJP, cored a sequence of subaerially erupted volcaniclastic rocks at least 338 m thick (Mahoney *et al.* 2001).

Ocean Drilling Program Leg 192, Site 1184

The volcaniclastic sequence at Site 1184 was divided into six subunits (Subunits IIA–IIF;

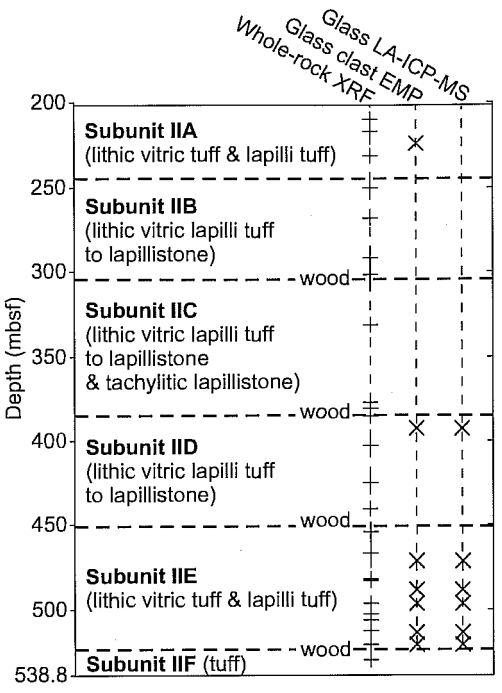

Fig. 2. Simplified section through the volcaniclastic succession at 1184A, showing the thicknesses and *dominant* lithological characteristics (see Thordarson 2004 for more details) of Subunits IIA–IIF, and stratigraphic positions of samples analysed for this study. Stratigraphic positions of wood fragments are also indicated.

Fig. 2) based on sedimentological and chemical characteristics (Fitton & Godard 2004; Thordarson 2004). Lithological features of the Site 1184 rocks are described by Mahoney *et al.* (2001) and Thordarson (2004), and the rocks are interpreted as primary hydromagmatic deposits from Surtseyan eruptions. The sequence consists predominantly of massive coarse lithic vitric tuffs, lapilli tuffs and lapillistones. The existence of blocky, subangular, non-vesicular glass shards implies that the eruptions were phreatomagmatic, and abundant accretionary lapilli indicate that the eruptions formed subaerial eruption columns. Many intervals contain basaltic lithic clasts (see Shafer *et al.* 2004). The presence of wood fragments at the top of Subunits IIC, IID, IIE and IIF shows that parts of the eastern salient formed emergent islands at the time of eruption. Discrete mineral grains (plagioclase and pyroxene) are a volumetrically minor component, and the tuffs are cemented with zeolites or calcite. Glass shards, abundant in Subunits IIA, IIB, IID and IIE, are thought to represent the juvenile magmas that were quenched during these hydroclastic eruptions. Although in general the sequence is heavily altered, some intervals contain glass clasts with unaltered centres.

Site 1184 was chosen to be near the summit of the northern ridge of the eastern salient, a location that may have originally been at relatively shallow water depths. Prior to drilling at Site 1184, the relationship between the eastern salient and the high plateau was unknown. The eastern salient has been proposed as: (1) part of the main plateau (Mahoney *et al.* 2001); (2) belonging to a postulated plume tail (Mahoney *et al.* 2001); (3) a younger section of the plateau formed in response to a change in the stress field of the plateau associated with a major change in Pacific plate motion at approximately 43 Ma (Duncan & Clague 1985); (4) the main locus of approximately 90 Ma volcanism (Tejada *et al.* 1996); or (5) a younger volcanic constructional feature related to passage of the plateau over the Samoan hot spot at *c.* 35–40 Ma (Yan & Kroenke 1993), and which may have also been recorded on Makira (Birkhold 2000). Thus, the presence of a thick volcaniclastic sequence in the eastern salient was surprising.

Biostratigraphical evidence collected during Leg 192 suggested that the basement at Sites 1183, 1185, 1186 and 1187 is Aptian in age, with a 125 m-thick carapace of overlying 'Kroenke-type' basalts at Site 1185 having a poorly constrained age of Cenomanian–Albian (Mahoney *et al.* 2001). However, $^{40}Ar/^{39}Ar$ dating of these basalts (Chambers *et al.* 2002) shows no evidence that the basaltic carapace at Site 1185 is significantly younger than the underlying lavas: all of the basalts sampled during Leg 192 were emplaced during one magmatic event at about 120 Ma (range: 122.0 ± 1.9–105.5 ± 3.9 Ma (1σ)), with no evidence for a volumetrically significant younger phase at *c.* 90 Ma, as had been suggested by previous work (e.g. Mahoney *et al.* 1993; Tejada *et al.* 1996). At Site 1184, shipboard nannofossil data suggested that the volcaniclastic sequence was emplaced during the middle Eocene. However, the weighted mean of six total fusion $^{40}Ar/^{39}Ar$ ages on discrete feldspar crystals is 123.5 ± 1.8 Ma (1σ: Chambers *et al.* 2004), and a study of the volcaniclastic lithologies by Thordarson (2004) suggests that the volcaniclastic rocks are syn-eruption accumulations. Thus, in contrast to the biostratigraphic data, the $^{40}Ar/^{39}Ar$ and lithological evidence point to eruption and emplacement of the volcaniclastic rocks during the main Aptian plateau-building magmatic event. This is

supported by a steep palaeomagnetic inclination, consistent with a Cretaceous age (Riisager *et al.* 2004).

It is important to verify that the Site 1184 volcaniclastic rocks are compositionally similar to the main plateau-building basalts because, if so, this would be the first confirmed instance of substantial subaerial eruptions occurring as part of the OJP-forming magmatic event. This has implications for our understanding of the origin of the OJP and its environmental effects. In this paper, we present major- and trace-element data for samples of unaltered glass from clasts in volcaniclastic rocks at Site 1184, and Sr-, Nd- and Pb-isotopic data for bulk tuff samples. The chemical data are compared with whole-rock elemental data for basalts from the Ontong Java Plateau (Fitton & Godard 2004) to investigate any degree of compositional similarity. In addition, a comparison of the major-element data for unaltered glass and altered bulk tuff samples, as well as isotopic data for altered volcaniclastic rocks and basalts from the OJP (cf. Mahoney *et al.* 1993; Tejada *et al.* 1996, 2002, 2004; Neal *et al.* 1997), provide some constraints on the chemical and isotopic changes that occur during sedimentation and alteration, and may assist future studies of similarly altered volcaniclastic rocks. This work is complemented by a study of lithic clasts from the volcaniclastic rocks at Site 1184 (Shafer *et al.* 2004).

Analytical methods

For analysis of glass clasts, shipboard samples were taken at intervals where hand-specimen examination indicated that unaltered glass was present: criteria for determining this included conchoidal fracture, a vitreous lustre and hardness exceeding that of a steel probe. Subunits IIB and IIC of the volcaniclastic succession at Site 1184 did not contain unaltered glass, and clasts from Subunit IIA were heavily fractured. Thus, the samples are biased towards Subunit IIE, reflecting the increasing glass preservation with depth in the core.

To separate glass clasts for laser ablation inductively coupled plasma-mass spectrometry (LA-ICP-MS), samples were soaked in water, subjected to repeated freeze–thaw action over several weeks and then gently crushed using a fly press. Hand-picked, cleaned, intact glass fragments large enough for LA-ICP-MS analysis were obtained from Subunits IID and IIE. Polished epoxy grain mounts were prepared; the smooth surface helps prevent the build-up of ablated particles. LA-ICP-MS analyses were conducted at the University of Notre Dame using a PlasmaQuad II STE quadrupole ICP-MS and a Nd-YAG laser quadrupled to 266 nm. Power used for these analyses was *c.* 0.9 mJ with a spot size of *c.* 25 μm and a repetition rate of 4 Hz. Tuning and standardization was conducted using NIST612 standard glass (cf. Pearce *et al.* 1997). Data reduction was achieved using the LAMTRACE program of Simon Jackson (MacQuarie University). Each sample was analysed twice. The standard NIST612 glass was analysed twice at the beginning and twice at the end of each analytical run, and was also analysed as an unknown during the run as a check of analytical precision and machine stability. Electron microprobe data from the University of Leicester (see below) were used as internal standards.

Polished thin sections were prepared for electron microprobe analysis. This approach was preferred as it minimized any bias towards particular morphologies during picking of glass fragments, and eliminated any risk of mixing grains between samples. Major- and minor-element compositions were determined on a JEOL 8600 electron microprobe at the University of Leicester using a 15 kV accelerating voltage, a 30 nA beam current and a 20 μm-diameter beam. This beam diameter was chosen to be small enough to avoid inclusions and/or heterogeneities in the glass clasts, whilst being large enough to minimize loss of the more volatile elements, notably Na, during analysis. Count times were 20 s on the peak and background for Si, Ti, Al, Fe, Mg, Ca, Na and K. The raw data were corrected using a ZAF (atomic number, absorption, fluorescence) correction procedure.

Whole-rock major- and trace-element data for the bulk tuff samples were analysed by X-ray fluorescence (XRF) at the University of Edinburgh and by ICP-MS using a VG-PQ2 Turbo+ spectrometer at ISTEEM, Montpellier; data and analytical details are reported in Fitton & Godard (2004). Four bulk tuff samples, representing the range of trace-element characteristics of the volcaniclastic rocks, were analysed for Sr-, Nd- and Pb-isotopic composition at the Scripps Institution of Oceanography using the procedure described in Tejada *et al.* (2004; see also Janney & Castillo 1996, 1997). For detailed descriptions of the lithologies from which these samples were taken, see Mahoney *et al.* (2001) and Thordarson (2004). Powders of samples analysed for Sr- and Nd-isotopic ratios were first leached in 4.5 N HCl to mitigate the effects of sea-water alteration (e.g. Mahoney 1987; Janney & Castillo 1996, 1997; Tejada *et al.* 2004); those for Pb-isotopic ratios were not leached because it was suspected that the majority of the Pb was in a leachable phase.

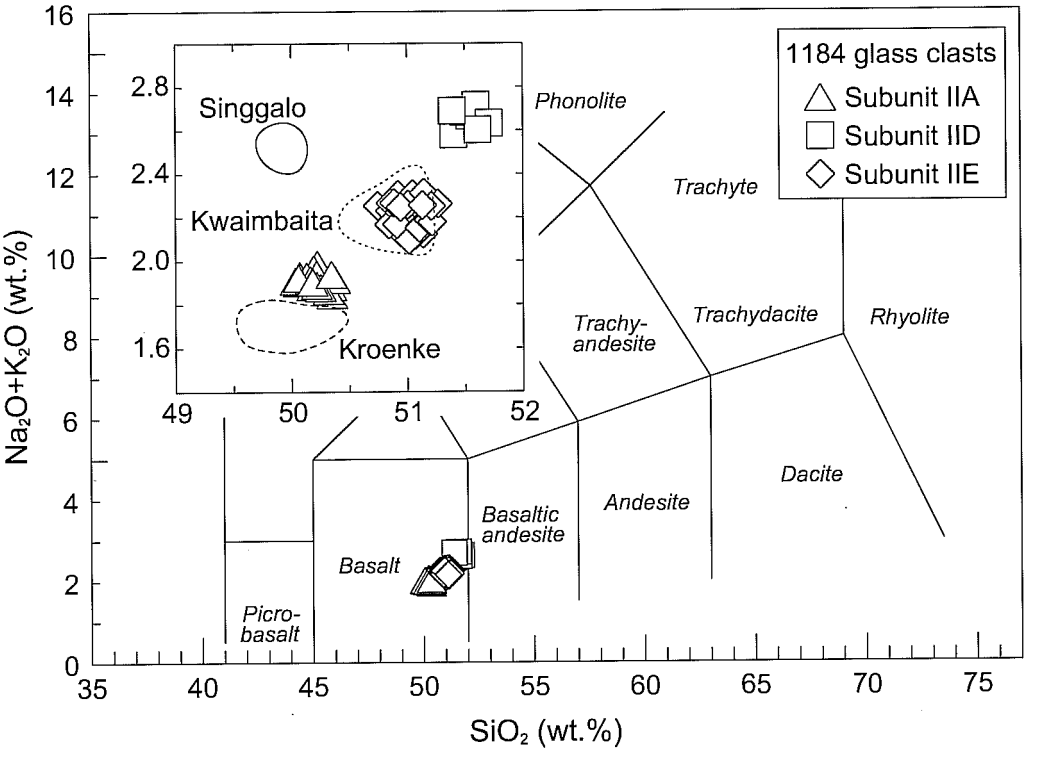

Fig. 3. Total alkalis v. silica plot for glass clasts analysed by electron microprobe (EMP), compared with fields for Kwaimbaita-, Kroenke- and Singgalo-type basalts from the OJP (data for basalts with LOI<0.5 wt% from Fitton & Godard 2004).

Results

Major-element compositions of glass clasts

All of the glass clasts analysed are basaltic low-K tholeiites (Fig. 3, Table 1), with approximately 49.5–51 wt% SiO_2, 6.5–9 wt% MgO and K_2O < 0.2 wt%. Data from all seven samples define three distinct compositional sets, corresponding perfectly to Subunits IIA, IID and IIE. This suggests that volcanic and sedimentary processes did not rework and mix glass populations, and supports the hypothesis that the glass clasts represent the juvenile magmatic component of the volcanic eruptions driving the emplacement of the volcaniclastic sequence (Thordarson 2004).

The uppermost subunit, Subunit IIA, has the most primitive magma composition, with an average MgO content of 9.0 wt% and average TiO_2 of 0.9 wt%. The least primitive compositions are present in Subunit IID, with average MgO of 6.7 wt% and average TiO_2 of 1.3 wt%. Subunit IIE has intermediate compositions, with average MgO of 7.9 wt% and average TiO_2 of 1.0 wt%.

Comparison with OJP basalt compositions. Three distinct basalt types are now recognized on the OJP (for details see Fitton & Godard 2004): (1) abundant Kwaimbaita-type basalts, typically with 6–8 wt% MgO; (2) Kroenke-type basalts, first described during ODP Leg 192, with MgO contents up to 11 wt%; and (3) Singgalo-type basalts, with similar MgO contents to Kwaimbaita-type basalts, but distinct Sr–Nd–Pb isotope ratios from both Kwaimbaita- and Kroenke-type basalts. Figure 4 compares glass clast compositions (open symbols) with fields for OJP Kwaimbaita-, Kroenke- and Singgalo-type basalts that have loss on ignition (LOI) of less than 1% (Fitton & Godard 2004). No Singgalo-type basalts were recovered during Leg 192; those reported by Fitton and Goddard (2004) are from ODP Leg 130 Site 807. Data for Site 1184 bulk tuff samples with LOI ranging

Table 1. *Electron microprobe data (wt%) for glass clasts from Site 1184, Subunits IIA, IID and IIE*

Analysis No.	SiO_2	TiO_2	Al_2O_3	FeO	MnO	MgO	CaO	Na_2O	K_2O	Total
1184A 13R-3, 142–148 cm (224.49 mbsf) Subunit IIA										
RVW022: 31	49.76	0.84	14.92	9.63	0.17	8.84	13.33	1.79	0.08	99.36
RVW022: 32	49.94	0.89	14.71	9.64	0.14	8.99	13.05	1.77	0.06	99.19
RVW022: 33	49.93	0.85	14.85	9.44	0.20	8.95	13.15	1.80	0.09	99.26
RVW022: 34	49.74	0.84	14.74	9.46	0.15	9.02	13.12	1.77	0.07	98.91
RVW022: 36	49.91	0.87	14.81	9.57	0.18	8.98	13.07	1.79	0.08	99.26
RVW022: 37	49.93	0.88	14.83	9.52	0.16	9.01	13.12	1.79	0.08	99.32
RVW022: 38	49.66	0.87	14.74	9.21	0.18	9.01	13.10	1.71	0.09	98.57
RVW022: 39	50.03	0.89	14.72	9.58	0.19	8.83	13.14	1.77	0.08	99.23
RVW022: 41	49.82	0.89	14.79	9.47	0.14	8.76	13.30	1.87	0.08	99.12
RVW022: 42	49.70	0.86	14.81	9.44	0.16	9.04	12.90	1.74	0.08	98.73
RVW022: 43	49.84	0.88	14.85	9.52	0.15	8.98	13.11	1.85	0.08	99.26
RVW022: 44	49.82	0.86	14.75	9.64	0.14	9.01	13.16	1.77	0.08	99.23
RVW022: 45	49.84	0.90	14.79	9.63	0.17	8.78	13.28	1.82	0.08	99.29
RVW022: 46	49.73	0.91	14.95	9.53	0.18	8.95	13.11	1.78	0.09	99.23
RVW022: 47	49.98	0.90	14.77	9.59	0.20	9.03	13.09	1.78	0.09	99.43
RVW022: 48	49.79	0.85	14.86	9.30	0.16	9.04	13.26	1.78	0.10	99.14
RVW022: 49	49.74	0.88	14.77	9.27	0.17	8.92	13.10	1.77	0.10	98.72
RVW022: 50	49.95	0.89	14.91	9.33	0.21	9.02	13.15	1.81	0.10	99.37
RVW022: 51	50.04	0.93	14.88	9.43	0.19	9.05	13.16	1.77	0.08	99.53
RVW022: 52	49.71	0.89	14.78	9.53	0.18	9.03	13.16	1.83	0.07	99.18
RVW022: 53	49.95	0.88	14.89	9.62	0.15	8.99	13.28	1.83	0.07	99.66
RVW022: 55	49.81	0.84	14.84	9.66	0.17	9.18	13.08	1.81	0.07	99.46
RVW022: 56	49.99	0.92	14.86	9.51	0.19	8.78	13.34	1.78	0.08	99.45
RVW022: 57	49.97	0.87	14.82	9.49	0.12	9.11	13.14	1.78	0.10	99.40
RVW022: 58	50.01	0.86	14.89	9.65	0.23	9.04	13.21	1.82	0.08	99.79
RVW022: 59	49.85	0.91	14.80	9.55	0.18	8.97	13.16	1.77	0.10	99.29
RVW022: 60	49.88	0.83	14.79	9.34	0.18	8.93	13.17	1.81	0.09	99.02
Average	**49.86**	**0.88**	**14.82**	**9.50**	**0.17**	**8.97**	**13.16**	**1.79**	**0.08**	**99.24**
1184A 31R-7 53–58 cm (392.85 mbsf) Subunit IID										
RVW020: 05	50.67	1.30	13.26	12.29	0.22	6.78	11.12	2.47	0.15	98.26
RVW020: 06	50.69	1.22	13.29	12.18	0.24	6.61	11.13	2.46	0.12	97.94
RVW020: 07	50.66	1.31	13.27	12.27	0.21	6.68	11.29	2.49	0.15	98.33
RVW020: 08	50.60	1.39	13.30	12.52	0.24	6.71	11.12	2.41	0.13	98.42
RVW020: 09	50.78	1.28	13.23	12.49	0.19	6.69	11.09	2.43	0.13	98.31
RVW020: 10	50.57	1.24	13.24	12.27	0.23	6.68	11.09	2.52	0.14	97.98
RVW020: 11	50.46	1.38	13.29	12.20	0.28	6.72	11.19	2.50	0.14	98.16
Average	**50.63**	**1.30**	**13.27**	**12.32**	**0.23**	**6.70**	**11.15**	**2.47**	**0.14**	**98.20**
1184A 39R-7, 95–99 cm (471.62 mbsf) Subunit IIE										
RVW021: 01	50.09	1.02	14.02	10.35	0.16	7.83	12.74	2.10	0.12	98.43
RVW021: 06	49.97	1.04	13.90	10.23	0.17	7.75	12.43	2.00	0.12	97.62
RVW021: 07	49.77	1.06	13.94	10.14	0.18	7.75	12.61	2.04	0.10	97.60
RVW021: 15	49.73	1.03	13.90	10.23	0.25	7.88	12.36	2.01	0.08	97.46
RVW021: 16	49.52	0.99	13.85	10.27	0.14	7.82	12.50	2.04	0.09	97.22
Average	**49.82**	**1.03**	**13.92**	**10.24**	**0.18**	**7.81**	**12.53**	**2.04**	**0.10**	**97.67**
1184A 41R-6, 67–72 cm (488.72 mbsf) Subunit IIE										
RVW020: 21	50.68	1.06	14.14	10.49	0.21	7.91	12.63	2.11	0.10	99.33
RVW020: 22	50.91	1.04	14.29	10.68	0.13	8.09	12.67	2.09	0.12	100.02
RVW020: 23	50.41	0.97	14.06	10.57	0.19	7.95	12.43	2.06	0.12	98.76
RVW020: 25	51.09	0.99	14.29	10.54	0.17	8.04	12.58	2.07	0.10	99.87
RVW020: 27	51.16	1.10	14.20	10.60	0.23	8.00	12.68	2.10	0.11	100.18
RVW020: 28	50.81	1.01	14.19	10.47	0.13	7.87	12.59	2.08	0.10	99.25
RVW020: 29	50.64	1.02	14.22	10.74	0.18	8.00	12.67	2.15	0.10	99.72
Average	**50.81**	**1.03**	**14.20**	**10.58**	**0.18**	**7.98**	**12.61**	**2.09**	**0.11**	**99.59**
1184A 42R-5, 69–74 cm (496.93 mbsf) Subunit IIE										
RVW021: 23	50.20	1.07	14.01	10.45	0.18	7.96	12.48	2.10	0.10	98.56
RVW021: 24	50.09	0.92	14.04	10.48	0.17	7.88	12.47	2.08	0.10	98.23
RVW021: 26	50.16	0.99	13.84	10.49	0.24	7.86	12.37	1.99	0.10	98.04
RVW021: 27	50.36	1.16	14.09	10.33	0.17	7.85	12.27	2.03	0.11	98.36
RVW021: 30	50.23	1.05	14.07	10.47	0.23	7.97	12.28	2.06	0.11	98.47
Average	**50.21**	**1.04**	**14.01**	**10.44**	**0.20**	**7.91**	**12.37**	**2.05**	**0.10**	**98.33**

Table 1. *continued*

Analysis No.	SiO_2	TiO_2	Al_2O_3	FeO	MnO	MgO	CaO	Na_2O	K_2O	Total
1184A 44R-3, 78–83 cm (513.53 mbsf) Subunit IIE										
RVW022: 02	50.83	1.04	14.27	10.69	0.16	8.04	12.57	2.10	0.08	99.78
RVW022: 03	50.81	1.02	14.34	10.58	0.14	8.10	12.46	2.12	0.11	99.68
RVW022: 06	50.62	1.04	14.25	10.34	0.16	8.33	12.30	2.17	0.12	99.33
RVW022: 07	50.74	1.01	14.21	10.48	0.17	8.12	12.44	2.14	0.09	99.40
RVW022: 09	50.84	1.02	14.27	10.49	0.17	8.04	12.40	2.12	0.09	99.44
RVW022: 10	50.89	1.01	14.21	10.73	0.16	8.10	12.38	2.04	0.09	99.61
RVW022: 11	50.75	1.01	14.27	10.68	0.22	8.08	12.41	2.08	0.10	99.60
RVW022: 13	50.59	1.06	14.18	10.47	0.16	7.99	12.62	2.06	0.11	99.24
RVW022: 14	50.83	0.98	14.20	10.40	0.13	8.03	12.53	2.11	0.10	99.31
RVW022: 15	50.87	1.07	14.18	10.75	0.15	7.58	12.43	2.14	0.09	99.26
RVW022: 16	50.96	1.11	14.23	10.75	0.20	7.62	12.36	2.16	0.09	99.48
RVW022: 17	50.60	1.03	14.20	10.68	0.22	8.02	12.44	2.15	0.10	99.44
RVW022: 18	50.98	1.07	14.12	10.64	0.22	7.72	12.40	2.13	0.12	99.40
RVW022: 20	50.72	1.06	14.17	10.61	0.19	7.74	12.58	2.08	0.09	99.24
RVW022: 21	50.66	1.00	14.26	10.49	0.13	7.96	12.56	2.10	0.11	99.27
RVW022: 22	50.82	1.09	14.12	10.71	0.18	8.07	12.67	2.14	0.09	99.89
RVW022: 23	50.84	1.00	14.27	10.57	0.22	8.02	12.42	2.10	0.11	99.55
RVW022: 24	50.85	1.02	14.12	10.66	0.19	8.05	12.60	2.13	0.09	99.71
RVW022: 25	50.64	1.04	14.19	10.56	0.19	8.12	12.60	2.05	0.11	99.50
RVW022: 26	50.64	1.08	14.24	10.36	0.16	8.08	12.51	2.13	0.10	99.30
RVW022: 27	50.87	1.05	14.42	10.59	0.16	7.44	12.56	2.18	0.12	99.39
RVW022: 28	50.96	1.03	14.37	10.76	0.20	7.82	12.67	2.18	0.10	100.09
RVW022: 29	50.94	0.99	14.18	10.54	0.18	7.98	12.36	2.14	0.10	99.41
RVW022: 30	50.95	1.04	14.26	10.59	0.15	8.06	12.48	2.16	0.09	99.78
Average	**50.80**	**1.04**	**14.23**	**10.59**	**0.18**	**7.96**	**12.49**	**2.12**	**0.10**	**99.50**
1184A 45R-2, 75–81 cm (521.40 mbsf) Subunit IIE										
RVW020: 32	50.86	0.91	14.33	10.60	0.21	8.13	12.52	2.13	0.11	99.80
RVW020: 33	51.05	1.08	14.27	10.77	0.20	8.02	12.51	2.10	0.10	100.10
RVW020: 37	50.47	0.95	14.02	10.45	0.20	8.00	12.44	2.11	0.09	98.73
RVW020: 40	51.13	0.94	14.34	10.64	0.18	8.05	12.57	2.19	0.12	100.16
RVW022: 61	50.18	1.03	14.00	10.60	0.17	7.91	12.42	2.02	0.08	98.41
RVW022: 62	50.27	1.00	14.06	10.51	0.19	7.89	12.38	2.06	0.10	98.46
RVW022: 66	50.12	1.01	14.04	10.33	0.23	7.88	12.51	1.98	0.08	98.18
RVW022: 67	50.31	1.00	13.97	10.42	0.19	7.96	12.36	2.05	0.11	98.37
RVW022: 68	50.29	1.04	13.99	10.28	0.20	7.94	12.45	2.05	0.11	98.35
RVW022: 69	50.37	1.05	13.97	10.28	0.18	7.92	12.66	2.01	0.08	98.52
RVW022: 70	50.37	1.00	14.01	10.33	0.18	8.04	12.40	2.07	0.10	98.50
RVW022: 71	50.44	1.04	14.10	10.49	0.19	7.96	12.34	2.09	0.12	98.77
RVW022: 73	50.35	1.07	13.96	10.53	0.20	7.99	12.27	2.12	0.11	98.60
RVW022: 74	50.32	1.03	14.06	10.36	0.20	7.89	12.29	2.10	0.12	98.37
RVW022: 75	49.80	1.04	13.95	10.35	0.18	7.87	12.44	2.13	0.09	97.85
RVW022: 76	50.34	1.07	13.97	10.53	0.22	7.96	12.36	2.05	0.11	98.61
RVW022: 77	50.20	1.05	13.97	10.49	0.17	7.87	12.42	2.07	0.10	98.34
RVW022: 78	50.40	1.08	14.01	10.61	0.20	7.90	12.32	2.04	0.10	98.66
RVW022: 79	50.14	1.01	14.00	10.42	0.20	7.94	12.49	2.10	0.09	98.39
RVW022: 80	50.11	1.05	13.98	10.44	0.16	7.95	12.50	2.04	0.10	98.33
RVW022: 81	50.30	1.01	13.97	10.55	0.16	7.94	12.28	2.04	0.11	98.36
RVW022: 82	50.27	1.04	14.13	10.41	0.23	7.96	12.47	2.13	0.11	98.75
RVW022: 83	50.37	1.03	14.01	10.48	0.14	7.96	12.43	2.06	0.08	98.56
RVW022: 84	50.22	1.04	14.00	10.44	0.22	7.99	12.49	2.06	0.08	98.54
RVW022: 85	49.93	1.04	13.89	10.12	0.21	7.90	12.49	1.99	0.12	97.69
RVW022: 86	50.25	1.02	14.04	10.28	0.21	7.86	12.43	2.03	0.09	98.21
RVW022: 87	50.53	1.04	14.01	10.73	0.24	7.93	12.39	2.13	0.10	99.10
RVW022: 88	50.54	1.00	13.92	10.56	0.14	7.90	12.41	2.06	0.10	98.63
RVW022: 89	50.30	0.99	14.01	10.23	0.18	7.96	12.34	2.05	0.09	98.15
RVW022: 90	50.35	1.07	14.01	10.46	0.20	7.97	12.32	2.03	0.09	98.50
Average	**50.35**	**1.02**	**14.03**	**10.46**	**0.19**	**7.95**	**12.42**	**2.07**	**0.10**	**98.60**

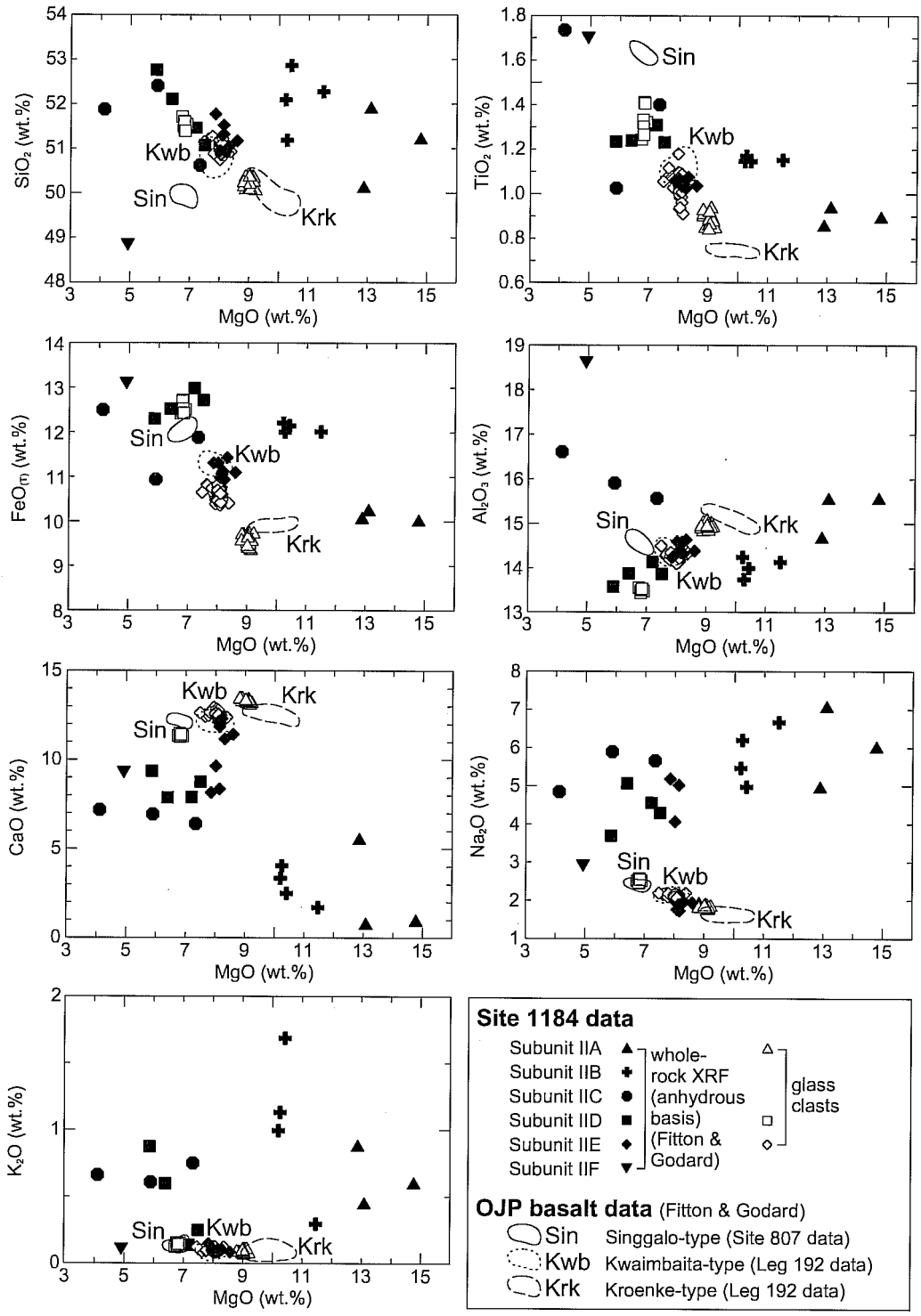

Fig. 4. Major-element plots v. MgO, comparing EMP data from glass clasts, whole-rock data for OJP basalts (reported on anhydrous basis, from analyses with <0.5 wt% LOI: Fitton & Godard 2004) and whole-rock data for Site 1184 bulk tuff samples (Fitton & Godard 2004), recalculated on an anhydrous basis with all Fe as FeO.

from 5 to 10% are included for comparison (closed symbols; Fitton & Godard 2004, recalculated on an anhydrous basis).

The glass from Subunit IIA (hereafter 'IIA glass') is broadly similar to the lower-MgO end of the Kroenke-type basalts. However, the IIA glass has marginally higher TiO_2, CaO and Na_2O, and marginally lower $FeO_{(T)}$ and Al_2O_3. In particular, the different TiO_2 contents for a given MgO content reflect subtle differences between the IIA glass and the Kroenke magma type.

Glass from Subunit IIE is very similar in composition to the widespread Kwaimbaita-type basalts of the OJP. The IIE glass has slightly lower $FeO_{(T)}$ contents, but there is good overlap with the Kwaimbaita field for all other elements analysed. Although Subunit IID glass has similar MgO, CaO, Na_2O and K_2O contents to the Singgalo-type magmas, the IID glass has significantly higher SiO_2, and significantly lower TiO_2 and Al_2O_3 contents.

In summary, the major-element compositions of glass clasts from Site 1184 support the hypothesis of a genetic relationship with the basalts of the high plateau. The predominant Kwaimbaita magma type appears to be present at Site 1184, and other Site 1184 magmas show varying degrees of similarity with other magma types recovered from the high plateau.

Comparison with Site 1184 bulk tuff compositions. Figure 4 demonstrates that the bulk tuff analyses differ substantially from analyses of unaltered glass from the centres of glass clasts. In particular, the processes of sedimentation, cementation and sea-water alteration have resulted in a marked depletion of CaO, and enrichment of Na_2O and K_2O relative to the unaltered glass (e.g. Hart *et al.* 1974; Verma 1992). In contrast, SiO_2, Al_2O_3, TiO_2 and $FeO_{(T)}$ have remained relatively unaffected. Not all subunits have been affected in the same way, e.g. MgO contents in Subunit IIA bulk tuffs are elevated by approximately 4 wt% relative to the unaltered IIA glass, whereas Subunit IID and IIE bulk tuffs are similar to those of the equivalent glass clasts. This difference in behaviour probably reflects changes in alteration style and/or degree of cementation within the volcanic pile. Although some of the difference between glass and bulk tuff compositions may be due to variability in the proportions of lithic clasts and crystal fragments within the tuffs, these components are generally volumetrically minor (Thordarson 2004), and cannot account for significant compositional differences.

Comparison between glass and bulk tuff compositions enables some qualitative estimates to be made of how volcaniclastic sequences like that at Site 1184 can act as sources or sinks of particular elements in the oceanic environment. For example, the bulk tuff samples from Subunit IIA demonstrate significant elemental mobility: in particular, MgO, Na_2O and K_2O have been added to the volcanic pile and CaO has been removed.

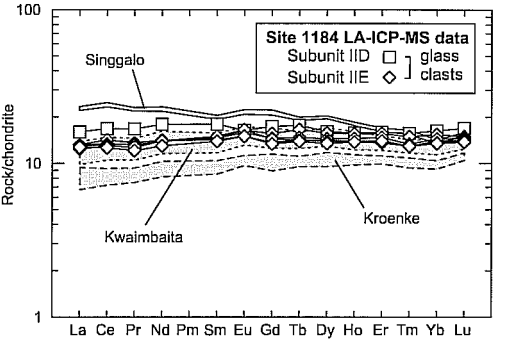

Fig. 5. Chondrite-normalized rare earth element (REE) plot (normalizing values from Sun & McDonough 1989) for Site 1184 glass clasts (LA-ICP-MS data) compared with fields for Kwaimbaita-, Kroenke- and Singgalo-type OJP basalts (data from Fitton & Godard 2004).

Incompatible trace-element compositions of glass clasts

Trace-element data for glass clasts are presented in Table 2, and plots of trace-element compositions are presented in Figures 5 and 6. Because of the uneven distribution of unaltered glass in Hole 1184A, there are five samples from Subunit IIE and only one sample from Subunit IID. Figures 5 and 6 demonstrate that the homogeneity in major-element composition amongst clasts from the same subunit (Subunit IIE) extends to incompatible trace elements as well. A difference in trace-element composition between Subunits IID and IIE is just discernible – the sample from Subunit IID has marginally higher incompatible trace-element contents, particularly for the highly incompatible elements, although the overall patterns are similar.

Comparison with trace-element data from basalts of the OJP (Fitton & Godard 2004) demonstrates that the Subunit IIE glass overlaps with the Kwaimbaita magma type in trace-element compositions. Glass from Subunit IID is marginally more enriched in a range of incompatible elements than Kwaimbaita-type magmas, but it is not enriched enough to resemble the Singgalo-type magmas (Fig. 7).

Table 2. *LA-ICP-MS data (ppm) for glass clasts from Site 1184, Subunits IID and IIE*

Site	1184A	1184A	1184A	1184A	1184A	1184A	NIST612	**NIST612**
Core Section	31R-7	39R-7	41R-6	42R-5	44R-3	45R-2	measured	**recommended**
Interval (cm)	53–58	95–99	67–72	69–74	78–83	75–81	average	**value**
Depth (mbsf)	392.85	471.62	488.72	496.93	513.53	521.40		
Subunit	IID	IIE	IIE	IIE	IIE	IIE		
V	359.9 ± 21.7	339.8 ± 12.9	305.7 ± 23.1	312.8 ± 28.3	330.1 ± 30.7	306.0 ± 21.8	38.54 ± 2.74	**39.22**
Cr	329.3 ± 6.6	372.8 ± 17.4	307.9 ± 10.7	325.8 ± 15.1	358.9 ± 31.8	321.2 ± 6.33	40.42 ± 7.96	**39.88**
Co	43.7 ± 11.43	53.75 ± 5.02	53.6 ± 4.74	54.5 ± 0.57	55.9 ± 3.61	40.1 ± 3.54	34.97 ± 3.09	**35.26**
Ga	14.7 ± 2.23	17.60 ± 1.90	18.0 ± 0.06	20.4 ± 0.26	20.4 ± 2.08	15.6 ± 1.08	36.97 ± 2.56	**36.24**
Rb	3.4 ± 0.09	2.39 ± 0.35	2.3 ± 0.01	2.3 ± 0.53	2.4 ± 0.21	1.70 ± 0.09	31.00 ± 1.65	**31.63**
Sr	96.8 ± 0.44	97.65 ± 0.80	103.6 ± 5.47	102.8 ± 6.10	103.3 ± 4.50	95.3 ± 3.76	76.14 ± 3.00	**76.15**
Y	23.9 ± 0.60	19.63 ± 0.81	20.0 ± 0.28	19.7 ± 0.14	19.0 ± 1.14	18.1 ± 0.65	38.09 ± 1.36	**38.25**
Zr	55.1 ± 2.59	47.22 ± 0.50	51.9 ± 0.85	51.7 ± 1.30	50.1 ± 2.29	50.3 ± 0.92	35.84 ± 0.66	**35.99**
Nb	3.70 ± 0.12	2.86 ± 0.27	3.19 ± 0.11	3.09 ± 0.15	3.15 ± 0.36	2.72 ± 0.08	38.10 ± 1.18	**38.06**
Cs	0.49 ± 0.15	0.38 ± 0.11	0.41 ± 0.12	0.34 ± 0.15	0.30 ± 0.05	0.51 ± 0.02	41.68 ± 1.68	**41.64**
Ba	21.2 ± 0.81	16.85 ± 1.27	17.8 ± 1.06	17.7 ± 0.14	17.1 ± 1.16	16.2 ± 0.51	37.71 ± 1.18	**37.74**
La	3.79 ± 0.13	3.13 ± 0.14	3.11 ± 0.19	3.06 ± 0.26	2.93 ± 0.09	3.01 ± 0.07	35.68 ± 0.81	**35.77**
Ce	10.29 ± 0.90	8.67 ± 0.70	8.21 ± 0.24	8.05 ± 0.09	7.93 ± 0.41	7.72 ± 0.23	38.22 ± 1.14	**38.35**
Pr	1.59 ± 0.02	1.29 ± 0.17	1.25 ± 0.00	1.20 ± 0.06	1.21 ± 0.06	1.15 ± 0.04	37.20 ± 1.24	**37.16**
Nd	8.38 ± 0.50	6.59 ± 0.02	6.49 ± 0.75	6.57 ± 0.33	6.53 ± 0.34	6.06 ± 0.19	35.25 ± 1.09	**35.24**
Sm	2.75 ± 0.38	2.17 ± 0.47	2.25 ± 0.13	2.23 ± 0.45	2.29 ± 0.54	2.13 ± 0.09	36.52 ± 1.53	**36.72**
Eu	0.95 ± 0.06	0.87 ± 0.00	0.95 ± 0.18	0.92 ± 0.04	0.96 ± 0.04	0.87 ± 0.01	34.35 ± 0.57	**34.44**
Gd	3.57 ± 0.43	2.81 ± 0.30	3.21 ± 0.12	2.99 ± 0.22	2.95 ± 0.29	2.75 ± 0.06	36.78 ± 0.79	**36.95**
Tb	0.66 ± 0.12	0.53 ± 0.05	0.62 ± 0.08	0.55 ± 0.02	0.53 ± 0.05	0.52 ± 0.01	35.88 ± 0.96	**35.92**
Dy	4.09 ± 0.22	3.59 ± 0.23	4.00 ± 0.30	3.67 ± 0.28	3.53 ± 0.03	3.42 ± 0.10	36.02 ± 1.10	**35.97**
Ho	0.89 ± 0.09	0.79 ± 0.07	0.88 ± 0.02	0.82 ± 0.05	0.78 ± 0.03	0.78 ± 0.02	37.94 ± 1.05	**37.87**
Er	2.64 ± 0.00	2.29 ± 0.07	2.59 ± 0.15	2.44 ± 0.07	2.25 ± 0.01	2.32 ± 0.06	37.31 ± 0.90	**37.43**
Tm	0.40 ± 0.04	0.33 ± 0.04	0.38 ± 0.00	0.34 ± 0.01	0.33 ± 0.05	0.33 ± 0.01	37.50 ± 1.17	**37.55**
Yb	2.77 ± 0.02	2.38 ± 0.07	2.62 ± 0.52	2.45 ± 0.23	2.32 ± 0.23	2.29 ± 0.08	39.94 ± 1.44	**39.95**
Lu	0.43 ± 0.09	0.36 ± 0.02	0.38 ± 0.02	0.37 ± 0.04	0.36 ± 0.03	0.35 ± 0.01	37.81 ± 1.06	**37.71**
Hf	1.65 ± 0.06	1.40 ± 0.07	1.55 ± 0.23	1.42 ± 0.10	1.42 ± 0.16	1.43 ± 0.05	34.62 ± 1.31	**34.77**
Ta	0.23 ± 0.03	0.18 ± 0.03	0.21 ± 0.03	0.20 ± 0.02	0.19 ± 0.02	0.19 ± 0.01	39.61 ± 1.78	**39.77**
Pb	0.60 ± 0.20	1.48 ± 0.04	0.76 ± 0.02	1.55 ± 0.52	1.45 ± 0.13	0.61 ± 0.04	38.80 ± 2.65	**38.96**
Th	0.28 ± 0.04	0.26 ± 0.03	0.25 ± 0.07	0.20 ± 0.05	0.27 ± 0.04	0.15 ± 0.01	37.46 ± 1.82	**37.23**
U	0.10 ± 0.04	0.08 ± 0.04	0.08 ± 0.01	0.11 ± 0.04	0.09 ± 0.00	0.08 ± 0.01	37.31 ± 3.82	**37.15**

Errors (all reported at 2σ) are calculated on the basis of duplicate analyses and the reproducibility of the NIST612 standard glass.
The NIST612 average data are on the basis of eight analyses.

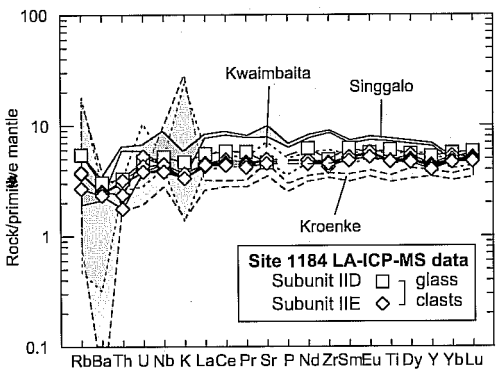

Fig. 6. Primitive-mantle-normalized multi-element diagram (normalizing values from Sun & McDonough 1989) for Site 1184 glass clasts (LA-ICP-MS data) compared with fields for Kwaimbaita-, Kroenke- and Singgalo-type OJP basalts (data from Fitton & Godard 2004).

Sr, Nd and Pb isotope compositions of bulk tuff samples

The ubiquitous presence of altered rims on the glass clasts made it impossible to obtain sufficient fresh glass for Sr-, Nd- and Pb-isotopic analysis, and, thus, four bulk tuff samples were analysed to verify the relationship between the variably altered volcaniclastic sequence at Site 1184 and Leg 192 lavas at Sites 1183, 1185, 1186 and 1187. The analyses are presented in Table 3 and Figure 8. Epsilon Nd values discussed in this section are initial values, calculated assuming an age of 120 Ma (denoted $\varepsilon_{Nd(t = 120\ Ma)}$).

Sample 1184A-11R-3, 28–34 cm has the highest $^{87}Sr/^{86}Sr$ and lowest $^{143}Nd/^{144}Nd$ among the samples. It has an $\varepsilon_{Nd(t = 120\ Ma)}$ that is slightly lower than those of the Leg 192 lavas ($\varepsilon_{Nd(t = 120\ Ma)}$ = 5.8–6.5: Tejada *et al.* 2004) and individual basaltic lithic clasts in the volcaniclastic sequence at Site 1184 ($\varepsilon_{Nd(t = 120\ Ma)}$ = 6.0–6.5:

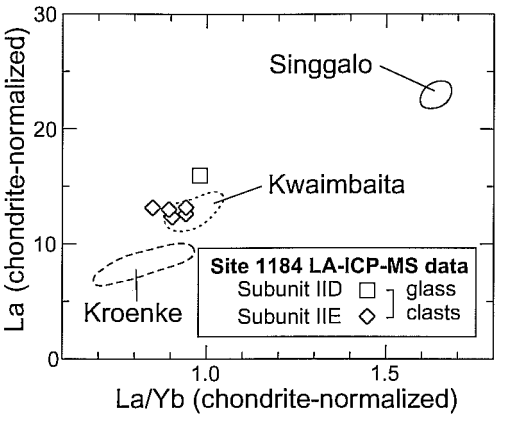

Fig. 7. Plot of La v. La/Yb (both chondrite normalized) for Site 1184 glass clasts (LA-ICP-MS data) compared with fields for Kwaimbaita-, Kroenke- and Singgalo-type OJP basalts (data from Fitton & Godard 2004).

Shafer *et al.* 2004), but falls within the range of previously analysed Kwaimbaita-type lavas (cf. Mahoney & Spencer 1991; Mahoney *et al.* 1993; Tejada *et al.* 1996, 2002; Neal *et al.* 1997). This sample belongs to Subunit IIA, which has a Kroenke-type elemental signature according to glass clasts and bulk tuff analyses. Kroenke-type lavas have a Kwaimbaita-type lava isotopic signature (Tejada *et al.* 2004). The Nd and Sr concentrations of sample 1184A-11R-3, 28–34 cm dropped dramatically after leaching (see table 4 of Fitton & Godard 2004 for unleached values), suggesting that most of its Sr and Nd contents are in the altered, leachable phases such as secondary phosphates and clay (e.g. Cheng *et al.* 1987; Mahoney & Spencer 1991; Janney & Castillo 1996, 1997). Thus, intense sea-water alteration is most probably responsible for its high $^{87}Sr/^{86}Sr$ (e.g. McCulloch *et al.* 1981; Cheng *et al.* 1987; Verma 1992). Sample 1184A-11R-3, 28–34 cm has lower Pb-isotopic ratios than the other samples analysed and all Ontong Java Plateau lavas; this is also probably due to intense sea-water alteration.

The $\varepsilon_{Nd(t\,=\,120\,Ma)}$ of sample 1184A-25R-5, 40–47 cm, from Subunit IIC, is within the ranges of Leg 192 Kwaimbaita-type lavas (Tejada *et al.* 2004) and lithic basaltic clasts from Site 1184 (Shafer *et al.* 2004). This is consistent with the similarity of most of the major- and trace-element contents of bulk tuff samples from this unit with Leg 192 Kwaimbaita-type lavas from Sites 1183, 1185 and 1186 (Fitton & Godard 2004). Age-corrected Sr- and Pb-isotopic ratios of the sample, however, are different from Leg 192 Kwaimbaita-type lavas. Although this sample is not as severely altered as sample 1184A-11R-3, 28–34 cm, its Sr- and Pb-isotope systematics may also have been modified by sea-water alteration.

Sample 1184A-42R-6, 7–18 cm is from Subunit IIE; the glass clasts from this subunit are compositionally homogeneous and overlap with the composition of Leg 192 Kwaimbaita-type lavas. The Sr-, Nd- and Pb-isotopic composition of sample 1184A-42R-6, 7–18 cm is very similar to that of Leg 192 lavas (Tejada *et al.* 2004) and overlaps with the field of the lithic basaltic clasts from Site 1184 (Shafer *et al.* 2004). It is important to note that this sample was chosen to be a geochemical reference sample for the volcaniclastic sequence at Site 1184 and, hence, was carefully chosen from the freshest section of the sequence. Sample 1184A-46R-1, 54–60 cm and the two other samples, on the other hand, were chosen not for freshness, but to cover the range of compositions.

Sample 1184A-46R-1, 54–60 cm, from Subunit IIF, has the highest Nd-isotopic ratios among the samples analysed. Consequently, it has higher $\varepsilon_{Nd(t\,=\,120\,Ma)}$ than all Leg 192 Kwaimbaita-type lavas and the lithic basaltic clasts from Site 1184. It also has high $^{207}Pb/^{204}Pb_{(pres.)}$ for a given $^{206}Pb/^{204}Pb_{(pres.)}$ ratio compared to Kwaimbaita- and Singgalo-type lavas, although not as high as the $^{207}Pb/^{204}Pb_{(pres.)}$ of the tuff layer above the basement at Site 1183 (15.563 v. 15.581: Tejada *et al.* 2004). Interestingly, the $^{206}Pb/^{204}Pb_{(pres.)}$, $^{208}Pb/^{204}Pb_{(pres.)}$ and $^{87}Sr/^{86}Sr_{(t\,=\,120\,Ma)}$ values overlap with Leg 192 Kwaimbaita-type lavas. Hence the majority of the isotopic signature of sample 1184A-46R-1, 54–60 cm is similar to that of Kwaimbaita-type lavas. A possible explanation for the isotopic composition of this sample is that it came from a source that has a slightly different composition (i.e. in Nd isotopes and $^{207}Pb/^{204}Pb$) from that of the Kwaimbaita-type lavas. More likely, its source is similar to that of the rest of Leg 192 lavas and volcaniclastic rocks, but its isotopic composition is variably affected by alteration.

In summary, the Nd-isotope signature of three out of four bulk tuff samples of the variably altered volcaniclastic sequence analysed is similar to that of the Kwaimbaita-type lavas; the Nd-isotope signature of the fourth sample is also close. The Pb-isotopic systematics are similar only to a limited degree and it is hard to predict their behaviour in the variably altered volcaniclastic rocks. The Sr-isotope systematics cannot be trusted as a petrogenetic tracer for the volcaniclastic sequence. That the Nd-isotope systematics of the volcaniclastic bulk tuff samples

Table 3. *Sr-, Nd- and Pb-isotopic composition of volcaniclastic rocks from ODP Site 1184*

Sample	$^{87}Sr/^{86}Sr$	$^{143}Nd/^{144}Nd$	$^{206}Pb/^{204}Pb$	$^{207}Pb/^{204}Pb$	$^{208}Pb/^{204}Pb$	Rb	Sr	Sm	Nd	U	Th	Pb	$^{87}Sr/^{86}Sr$	$^{143}Nd/^{144}Nd$	ε_{Nd}	$^{206}Pb/^{204}Pb$	$^{207}Pb/^{204}Pb$	$^{208}Pb/^{204}Pb$
	measured	–	–	–	–								120 Ma	–	–	–	–	–
1184A-11R-3, 28–34 cm																		
Subunit IIA	0.712880	0.512925	17.503	15.481	37.176	2.27	6.95	0.29	0.92	0.21	0.21	1.39	0.71127	0.512776	5.7	17.331	15.473	37.120
duplicate		0.512918						0.29	0.92					0.512769	5.5			
1184A-25R-5, 40–47 cm																		
Subunit IIC	0.704588	0.512981	17.653	15.520	37.481	0.56	9.03	0.79	2.12	0.15	0.54	1.92	0.70428	0.512805	6.2	17.564	15.516	37.376
1184A-42R-6, 7–18 cm																		
Subunit IIE	0.703948	0.512984	18.554	15.519	38.352	0.32	76.4	1.36	3.85	0.07	0.22	0.42	0.70393	0.512818	6.5	18.357	15.509	38.151
1184A-46R-1, 54–60 cm																		
Subunit IIF	0.703269	0.513032	18.658	15.563	38.417	0.36	50.4	0.62	1.84	0.38	0.83	1.27	0.70323	0.512873	7.5	18.306	15.546	38.165
duplicate (unleached)		0.513021						0.62	1.84					0.512862	7.3			

Sr- and Nd-isotope ratios were measured on leached powders. Analytical uncertainty for $^{87}Sr/^{86}Sr$ measurements is ±0.000018 but in-run precisions were better than ± 0.000013, except for sample1184A-11R-3, 28–34 cm, which was ± 0.000025. Sr-isotope ratios were measured by dynamic multi-collection, fractionation corrected to $^{86}Sr/^{88}Sr = 0.1194$ and normalized to $^{87}Sr/^{86}Sr = 0.71025$ for NBS 987. Analytical uncertainty for $^{143}Nd/^{144}Nd$ measurements is ±0.000014 (0.3 ε units) but in-run precisions were better than ±0.000012, except for the first run of sample1184A-11R-3, 28–34 cm, which was ± 0.000035. Nd-isotope ratios were measured in oxide form by dynamic multi-collection, fractionation corrected to $^{146}NdO/^{144}NdO = 0.72225$ ($^{146}Nd/^{144}Nd = 0.7219$) and are reported relative to $^{143}Nd/^{144}Nd = 0.511850$ for the La Jolla Standard. Pb-isotope ratios were measured by static multi-collection and are reported relative to the values of Todt *et al.* (1995) for NBS SRM 981; the long-term errors measured for this standard are ± 0.008 for $^{206}Pb/^{204}Pb$ and $^{207}Pb/^{204}Pb$, and ± 0.024 for $^{208}Pb/^{204}Pb$; the in-run precisions were better than this. Total procedural blanks are negligible: <10 picograms (pg) for Nd, <35 pg for Sr, <3 pg for Th, <5 pg for U and <60 pg for Pb. U, Th and Pb elemental concentrations used in the age-corrections for Pb-isotopes are given in the table. $\varepsilon_{Nd} = 0$ today corresponds to $^{143}Nd/^{144}Nd = 0.51264$; for $^{147}Sm/^{144}Nd = 0.1967$, $\varepsilon_{Nd}(t) = 0$ corresponds to $^{143}Nd/^{144}Nd = 0.512486$ at 120 Ma.

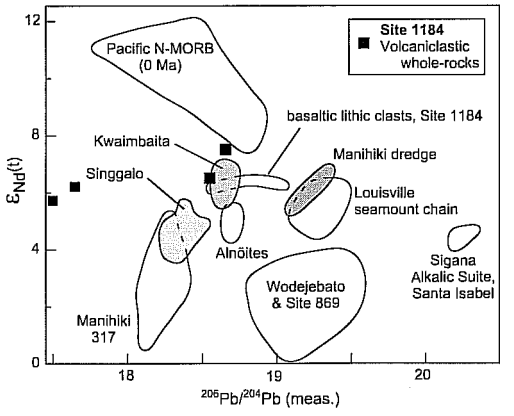

Fig. 8. Plot of ε_{Nd} v. $^{206}Pb/^{204}Pb$ for bulk tuff samples from Site 1184 compared with fields for previously analysed Kwaimbaita-, Singgalo-, Sigana-type and Alnöite lavas from the OJP (Mahoney & Spencer 1991; Tejada *et al.* 1996, 2002; Neal *et al.* 1997) and basaltic lithic clasts from Site 1184 (Shafer *et al.* 2004). Analytical error is smaller than the symbol used. Other fields shown are for the Louisville Seamount Chain, Manihiki Plateau (Mahoney 1987; Mahoney & Spencer 1991), Pacific normal-MORB (Tejada *et al.* 1996), and volcaniclastic rocks from ODP Site 869 and Wodejebato Guyot (Janney & Castillo 1999).

can be used as petrogenetic tracer for the source(s) of the volcanogenic components is also shown by results of isotopic investigations of the lithic basaltic clasts in the volcaniclastic sequence at Site 1184 (Shafer *et al.* 2004), the tuff layer above the lavas at Site 1183 (Tejada *et al.* 2004) and the volcaniclastic sequence in the Nauru Basin (Castillo 2004).

Discussion

Relationship between magma composition and stratigraphy

There is no consistent stratigraphic trend in composition between magma types that indicates evolution via magmatic differentiation processes, particularly fractional crystallization of a single magma batch. The glass clasts demonstrate that the earliest eruptions (Subunit IIE) were of a Kwaimbaita-type magma, followed by a more evolved magma (Subunit IID). The top of the succession (Subunit IIA) reverts to a more primitive magma type, similar to the Kroenke-type lavas of Sites 1185 and 1187. Furthermore, trace-element data for bulk tuff samples from all subunits of Hole 1184A show that at least five distinct magma compositions were erupted over the lifetime of the sampled portion of this volcano (Fitton & Godard 2004, fig. 7). The distribution of magma types relative to the stratigraphy indicates that the magma chamber was replenished with more primitive magma at least twice during the sampled time interval.

The dominance of Kwaimbaita- and Kroenke-type compositions in the glass clasts is consistent with observations made on the basaltic lithic clast population of the volcaniclastic rocks (Shafer *et al.* 2004). The modest heterogeneity observed at Site 1184 contrasts markedly with the majority of the OJP, in particular with the homogeneous Kwaimbaita-type magmas that dominate the sampled portions of the high plateau and the island of Malaita. The presence of complexly zoned plagioclase megacrysts (Babbs 1997) and plagioclase-rich xenoliths (Mahoney *et al.* 2001) in the Kwaimbaita-type lavas indicate that residence in magma chambers was responsible, at least in part, for this homogeneity. The juvenile components of the volcaniclastic sequence in the eastern salient of the OJP may not have had such an extensive magma storage system; alternatively, the explosivity of the eruptions may have tapped a wider range of magma compositions from a single magma reservoir, compared to effusive eruptions that may have only tapped the upper, well-mixed portion of the magma chamber (cf Kilauea: Dzurisin *et al.* 1995).

Extent of subaerial volcanism and implications for plume models

Confirming the presence and extent of volcaniclastic rocks that are part of the main plateau sequence may help to answer questions about the origin of the plateau and its subsidence history. Site 1184 has the only known example of near-source subaerially erupted volcaniclastic rocks on the OJP. Vitric tuff layers immediately above basement at DSDP Site 289 (Andrews *et al.* 1975) and ODP Site 1183 may represent shallow-water or subaerial eruptions, but these tuffs are considerably finer grained than the lapilli-dominated sequence at Site 1184, and the two layers at Site 1183 show evidence of sedimentary reworking (Mahoney *et al.* 2001). The loci of shallow-water or subaerial volcanic activity contributing to these vitric tuff layers remain unknown.

Consequently, the volume of volcaniclastic rocks making up the Ontong Java Plateau is extremely poorly constrained. Site 1184 is the

only site to have sampled 'basement' on the whole of the eastern salient, a feature that constitutes approximately a quarter of the area of the OJP (Fig. 1). Two-dimensional (2D) seismic surveys do not appear to discriminate effectively between basaltic and volcaniclastic basement, and therefore only further drilling will determine the extent of subaerial volcanic activity.

The presence of non-vesicular pillow basalts rather than subaerial lavas at the current topographic crest of the high plateau has created difficulties for the plume-head model of oceanic plateau generation (e.g. Richards *et al.* 1991), which predicts dynamic uplift of 1–3 km associated with the arrival of a plume head at the base of the lithosphere (e.g. Hill 1991). This amount of dynamic uplift, coupled with the relatively thin lithosphere thought to be required to explain the high degrees of partial melting (Mahoney *et al.* 1993; Tejada *et al.* 1996; Neal *et al.* 1997; Fitton & Godard 2004), and the thick plateau crust should have been sufficient to elevate the plateau crest above sea level during volcanism. Neal *et al.* (1997), however, point out that a hidden layer of high-density cumulates would have both limited uplift and tempered post-emplacement subsidence of the OJP.

The OJP has undergone subsidence of approximately 1.5 km since eruption of its youngest (sampled) lavas (Roberge *et al.* 2004*b*). This is considerably less than would be expected from the plume-head model combined with normal thermal subsidence. In spite of this problem, however, the plume-head model remains the most widely accepted hypothesis for the generation of the OJP, mainly because it is the only model amongst several contenders that adequately explains the generation of such a large magma volume derived from a relatively undepleted (i.e. non-mid-ocean ridge basalt) and volatile-poor (Roberge *et al.* 2004*a*) source in a relatively short period of time.

If the OJP *did* form above a plume head, and the apparent lack of subaerial volcanism on the high plateau is genuine, it suggests that our models of plume-generated uplift and/or plateau-related subsidence require re-evaluation. For example, if the anomalously hot mantle material rapidly flowed laterally during the plume impingement event, as has been suggested for the North Atlantic Igneous Province (Saunders *et al.* 1997; Larsen *et al.* 1999), the hot material could form a thinner, laterally more extensive sheet than is envisaged in many mantle plume models, and the amount of uplift would be lower. Alternatively, modelling by Olson (1994) suggests that if a plume head is emplaced beneath the lithosphere as a solitary thermal diapir rather than continuing to be fed from beneath, maximum topographic uplift would precede the peak of volcanism by about 5 Ma, and by the time the final lavas were emplaced (i.e. those that are sampled by ocean drilling) the plateau could have already undergone significant subsidence due to the withdrawal of dynamic support. In this case, any subaerial lavas and/or volcaniclastic successions would be buried beneath a carapace of younger, submarine lavas. On the high plateau, drilling has only penetrated the uppermost 217 m of the 30–35 km-thick crust, so it is possible that subaerial lithologies remain hidden underneath.

However, other oceanic plateaus do contain subaerial lithologies close to the top of the volcanic stratigraphy (e.g. Caribbean Plateau: White 1999; Kerguelen: Coffin *et al.* 2000). This demonstrates that, whether or not subaerial rocks exist deeper within the volcanic pile of the OJP, its mode of formation may have been different from those of other Cretaceous Pacific plateaus such as the Caribbean Plateau. The presence of a high-density cumulate layer within the OJP, as modelled by Neal *et al.* (1997), may be one of the more significant dissimilarities between the OJP and other Pacific oceanic plateaus.

Environmental and climatic implications

The OJP represents an immense outpouring of magma, but there is no significant mass extinction temporally associated with its eruption. This contrasts with the eruption of many continental flood basalt provinces, which correlate temporally with (and may have contributed to) major mass extinctions (e.g. Wignall 2001). A likely explanation for the lack of environmental catastrophe associated with the OJP is the observation that the majority of the volcanism occurred in the submarine environment, and that the magmas are relatively volatile-poor (Michael 1999; Roberge *et al.* 2004*a*). This would have restricted the flux of climate-affecting volatile species (e.g. SO_2, Cl, F, CO_2) into the atmosphere. However, our limited sampling of the OJP means that the proportion of subaerial volcanism, and thus the flux of volatiles associated with OJP magmatism, is very poorly constrained. It should also be noted that the likelihood of a mass extinction is not a simple function of volatile output of a volcanic system, as it depends on a web of interlinked factors combined with the ability of Earth's systems to withstand climatic and environmental perturbations (e.g. White 2002). Consequently, statements that assume a direct link between extinctions and volatile fluxes should be treated with caution.

Although the OJP does not correlate with any mass extinctions, it is temporally associated (Pringle 2001) with an environmental disturbance, recorded in the sedimentary and geochemical record as the Aptian Oceanic Anoxic Event 1a ('Selli Event'). At this time, black shale deposition was associated with a negative $\delta^{13}C$ excursion, a fall in sea-water $^{87}Sr/^{86}Sr$ and an increase in metal concentrations (Larson & Erba 1999). These environmental features are consistent with their being caused by large-scale basaltic volcanism, with increased volatile input into the atmosphere combined with increased hydrothermal fluxes into the oceans.

Conclusions

- The juvenile magmatic components of the volcaniclastic rocks recovered at Site 1184 are chemically and isotopically similar to pillow basalts and sheet flows recovered elsewhere on the OJP. This corroborates the hypothesis that the subaerial, explosive volcanism on the eastern salient of the OJP is part of the main early Aptian plateau-building magmatic event. In particular, the juvenile magmas contributing to Subunit IIE of Site 1184 are indistinguishable from Kwaimbaita-type magmas in terms of major- and trace-element composition, and are also similar in terms of Nd- and, to a limited extent, Pb-isotopic composition.
- Although all the glass clasts have a low-K tholeiitic composition, each of the three subunits that contain unaltered glass records a distinct juvenile magma composition. This suggests that the eastern salient had a different type of magma plumbing system to that of the high plateau, allowing a greater degree of heterogeneity to be preserved. No intermixing of glass clasts between subunits was detected, supporting the shipboard hypothesis (arising from the discovery of wood fragments at subunit boundaries) that each subunit represents a discrete eruptive phase with intervening periods of quiescence.
- Whereas drilling at Site 1185 indicated a hiatus between eruption of Kwaimbaita-type and Kroenke-type basalts, the volcaniclastic succession at Site 1184 indicates that both magma types were present within the lifetime of a single Surtseyan volcano, albeit one that had non-eruptive intervals of sufficient length for colonization by woody vegetation.
- Bulk tuff analyses for some samples closely match juvenile glass clast compositions from the same subunit, whereas others are markedly different. This reflects variability in the degree of alteration/cementation of the tuffs, and, to a lesser extent, the proportion of non-juvenile material (e.g. lithic clasts) incorporated into the sedimentary pile.
- At least some of the Ontong Java Plateau volcanism was subaerial, and thus had the potential to inject volatile, climate-modifying, species into the Cretaceous atmosphere. The volume of volcaniclastic rocks on the eastern salient (and elsewhere on the plateau), and thus the extent of these subaerial eruptive events, remains unquantified. Although the eruption of the OJP does not appear to have had a signifcant affect on contemporaneous biota, the magmatism does correspond temporally with the anoxic Selli Event.

This research used samples provided by the Ocean Drilling Program (ODP). ODP is sponsored by the U.S. National Science Foundation (NSF) and participating countries under management of Joint Oceanographic Institutions (JOI), Inc. We thank P. Janney and A. Pietruszka for their helpful reviews, R. Wilson for assistance with electron microprobe analyses, W. Kinman for help with the LA-ICP-MS analyses, and A. Saunders for informal discussions. R. V. White is supported by a Royal Society Dorothy Hodgkin Research Fellowship, and an ODP Rapid Response Grant from the Natural Environment Research Council (NERC). C. R. Neal was supported by a grant from USSSAC.

References

ANDREWS, J.E., PACKHAM, G.H. *et al.* 1975. Wellington, New Zealand to Apra Guam, April–June 1973. *Proceedings of the Deep Sea Drilling Project, Initial Reports*, **30**. College Station, TX, 753 pp.

BABBS, T.L. 1997. *Geochemical and petrological investigations of the deeper portions of the Ontong Java Plateau: Malaita, Solomon Islands.* PhD Thesis, University of Leicester.

BIRKHOLD, A.L. 2000. *A geochemical investigation of Ontong Java Plateau basement exposed on the Island of Makira (San Cristobal), Solomon Islands, South Pacific.* PhD Thesis, University of Notre Dame.

CASTILLO, P.R. 2004. Geochemistry of Cretaceous volcaniclastic sediments in the Nauru and East Mariana basins provides insights into the mantle sources of giant oceanic plateaus. *In*: FITTON, J.G., MAHONEY, J.J., WALLACE, P.J. & SAUNDERS, A.D. (eds) *Origin and Evolution of the Ontong Java Plateau.* Geological Society, London, Special Publications, **229**, 353–368.

CHAMBERS, L.M., PRINGLE, M.S. & FITTON, J.G. 2002. Age and duration of magmatism on the Ontong Java Plateau: ^{40}Ar–^{39}Ar results from ODP Leg 192. Abstract V71B-1271. *Eos, Transactions American Geophysical Union*, **83**, F47.

CHAMBERS, L.M., PRINGLE, M.S. & FITTON, J.G. 2004. Phreatomagmatic eruptions on the Ontong Java Plateau: an Aptian $^{40}Ar/^{39}Ar$ age for volcaniclastic rocks at ODP Site 1184. *In*: FITTON, J.G.,

MAHONEY, J.J., WALLACE, P.J. & SAUNDERS, A.D. (eds) *Origin and Evolution of the Ontong Java Plateau*. Geological Society, London, Special Publications, **229**, 325–331.

CHENG, Q., PARK, K.H., MACDOUGALL, J.D., ZINDLER, A., LUGMAIR, G.W., STAUDIGEL, H., HAWKINS, J.W. & LONSDALE, P.F. 1987. Isotopic evidence for a hotspot origin of the Louisville seamount chain. *In*: KEATING, B.H., FRYER, P., BATIZA, R. & BOEHLERT, G.W. (eds) *Seamounts, Islands, and Atolls*. American Geophysical Union, Geophysical Monograph, **43**, 283–296.

COFFIN, M.F., FREY, F.A. & WALLACE, P.J. 2000. *Proceedings of the Ocean Drilling Program, Initial Reports*, **183** (CD-ROM).

DUNCAN, R.A. & CLAGUE, D.A. 1985. Pacific Plate motion recorded by linear volcanic chains. *In*: NAIRN, A.E.M., STEHLI, F.G. & UYEDA, S. (eds) *The Ocean Basins and Margins: The Pacific Ocean*, vol. **7A**. Plenum, New York, 89–121.

DZURISIN, D., LOCKWOOD, J. P, CASADEVALL, T.J. & RUBIN, M. 1995. The Uwekahuna Ash Member of the Puna Basalt; product of violent phreatomagmatic eruptions at Kilauea Volcano, Hawaii, between 2800 and 2100 ^{14}C years ago. *Journal of Volcanology and Geothermal Research*, **66**, 163–184.

FITTON, J.G. & GODARD, M. 2004. Origin and evolution of magmas on the Ontong Java Plateau. *In*: FITTON, J.G., MAHONEY, J.J., WALLACE, P.J. & SAUNDERS, A.D. (eds) *Origin and Evolution of the Ontong Java Plateau*. Geological Society, London, Special Publications, **229**, 151–178.

GLADCZENKO, T.P., COFFIN, M.F. & ELDHOLM, O. 1997. Crustal structure of the Ontong Java Plateau: Modeling of new gravity and existing seismic data. *Journal of Geophysical Research*, **102**, 22 711–22 729.

HAGEN, R.A., MAYER, L.A., MOSHER, D.C., KROENKE, L.W., SHIPLEY, T.H. & WINTERER, E.L. 1993. Basement structure of the northern Ontong Java Plateau. *In*: BERGER, W.H., KROENKE, L.W. & MAYER, L.A. (eds) *Proceedings of the Ocean Drilling Program, Scientific Results*, **130**, 23–31.

HART, S.R., ERLANK, A.J. & KABLE, E.J.D. 1974. Seafloor basalt alteration: some chemical and Sr isotopic effects. *Contributions to Mineralogy and Petrology*, **44**, 219–230.

HILL, R.I. 1991. Starting plumes and continental break-up. *Earth and Planetary Science Letters*, **104**, 398–416.

JANNEY, P.E. & CASTILLO, P.R. 1996. Basalts from the Central Pacific Basin: Evidence for the origin of Cretaceous igneous complexes in the Jurassic Western Pacific. *Journal of Geophysical Research*, **101**, 2875–2894.

JANNEY, P.E. & CASTILLO, P.R. 1997. Geochemistry of Mesozoic Pacific MORB: constraints on melt generation and the evolution of the Pacific upper mantle. *Journal of Geophysical Research*, **102**, 5207–5229.

JANNEY, P.E. & CASTILLO, P.R. 1999. Isotope geochemistry of the Darwin Rise seamounts and the nature of long-term mantle dynamics beneath the south central Pacific. *Journal of Geophysical Research*, **104**, 10 571–10 589.

KROENKE, L.W. 1972. *Geology of the Ontong Java Plateau*. Hawaii Institute of Geophysics Report HIG, 72–75.

KROENKE, L.W., RESIG, J.M. & COOPER, P.A. 1986. Tectonics of the southeastern Solomon Islands: formation of the Malaita anticlinorium. *In*: VEDDER, J.G., POUND, K.S. & BOUNDY, S.Q. (eds) *Geology and Offshore Resources of Pacific Island Arcs – Central and Western Solomon Islands*. Circum-Pacific Council for Energy and Mineral Resources, Earth Science Series **4**, 109–116.

KROENKE, L.W., BERGER, W.H., JANECEK, T.R. *et al.* 1991. *Proceedings of the Ocean Drilling Program, Initial Results*, **130**.

LARSEN, T.B., YUEN, D.A. & STOREY, M.J. 1999. Ultrafast mantle plumes and implications for flood basalt volcanism in the Northern Atlantic Region. *Tectonophysics*, **311**, 31–43.

LARSON, R.L. & ERBA, E. 1999. Onset of the Mid-Cretaceous greenhouse in the Barremian–Aptian; igneous events and the biological, sedimentary, and geochemical responses. *Paleoceanography*, **14**, 663–678.

MAHONEY, J.J. 1987. An isotopic survey of Pacific ocean plateaus: implications for their nature and origin. *In*: KEATING, B.H., FRYER, P., BATIZA, R. & BOEHLERT, G.W. (eds) *Seamounts, Islands, and Atolls*. American Geophysical Union, Geophysical Monograph, **43**, 207–220.

MAHONEY, J.J. & SPENCER, K.J. 1991. Isotopic evidence for the origin of the Manihiki and Ontong Java oceanic plateaus. *Earth and Planetary Science Letters*, **104**, 196–210.

MAHONEY, J.J., STOREY, M., DUNCAN, R.A., SPENCER, K.J. & PRINGLE, M. 1993. Geochemistry and age of the Ontong Java Plateau. *In*: PRINGLE, M.S., SAGER, W.W., SLITER, W.V. & STEIN, S. (eds) *The Mesozoic Pacific: Geology, Tectonics, and Volcanism*. American Geophysical Union, Geophysical Monograph, **77**, 233–261.

MAHONEY, J.J., FITTON, J.G., WALLACE, P.J. *et al.* 2001. *Proceedings of the Ocean Drilling Program, Initial Reports*, **192** (CD-ROM).

MCCULLOCH, M.T., GREGORY, R.T., WASSERBURG, G.J. & TAYLOR, H.P., JR. 1981. Sm–Nd, Rb–Sr, and O-18/O-16 isotopic systematics in an oceanic crustal section; evidence from the Samail ophiolite. *In*: COLEMAN, R.G. & HOPSON, C.A. (eds) *Oman Ophiolite. Journal of Geophysical Research*, **86**, 2721–2735.

MICHAEL, P.J. 1999. Implications for magmatic processes at Ontong Java Plateau from volatile and major element contents of Cretaceous basalt glasses. *Geochemistry Geophysics Geosystems*, **1**, 1999GC000025.

NEAL, C.R., MAHONEY, J.J., KROENKE, L.W., DUNCAN, R.A. & PETTERSON, M.G. 1997. The Ontong Java Plateau. *In*: MAHONEY, J.J. & COFFIN, M.F. (eds) *Large Igneous Provinces: Continental, Oceanic, and Planetary Flood Volcanism*. American Geophysical Union, Geophysical Monograph, **100**, 183–216.

OLSON, P. 1994. Mechanics of flood basalt magmatism. *In*: RYAN, M.P. (ed.) *Magmatic Systems*. Academic Press, New York, 1–18.

PEARCE, N.J.G., PERKINS, W.T., WESTGATE, J.A.,

GORTON, M.P., JACKSON, S.E., NEAL, C.R. & CHERNERY, S.P. 1997. New data for the National Institute of Standards and Technology 610 and 612 glass reference materials. *Geostandards Newsletter*, **21**, 115–144.

PETTERSON, M.G., BABBS, T., NEAL, C.R., MAHONEY, J.J., SAUNDERS, A.D., DUNCAN, R.A., TOLIA, D., MAGU, R., QOPOTO, C., MAHOA, H. & NATOGGA, D. 1999. Geological-tectonic framework of Solomon Islands, SW Pacific: crustal accretion and growth within an intra-oceanic setting. *Tectonophysics*, **301**, 35–60.

PRINGLE, M.S. 2001. Revised age for Chron M0r implies synchronicity of volcanism on the Ontong Java Plateau with global oceanographic events. *Eos, Transactions of the American Geophysical Union*, **82**, Fall Meeting Supplement, Abstract T21D-09.

RICHARDS, M.A., JONES, D.L., DUNCAN, R.A. & DEPAOLO, D.J. 1991. A mantle plume initiation model for the Wrangellia flood basalt and other oceanic plateaus. *Science*, **254**, 263–267.

RICHARDSON, W.P., OKAL, E.A. & VAN DER LEE, S. 2000. Rayleigh-wave tomography of the Ontong-Java Plateau. *Physics of the Earth and Planetary Interiors*, **118**, 29–51.

RIISAGER, P., HALL, S., ANDRETTER, M. & ZHAO, X. 2004. Early Cretaceous Pacific palaeomagnetic pole from Ontong Java Plateau basement rocks. *In*: FITTON, J.G., MAHONEY, J.J., WALLACE, P.J. & SAUNDERS, A.D. (eds) *Origin and Evolution of the Ontong Java Plateau*. Geological Society, London, Special Publications, **229**, 31–44.

ROBERGE, J., WHITE, R.V. & WALLACE, P.J. 2004*a*. Volatiles in submarine basaltic glasses from the Ontong Java Plateau (ODP Leg 192): implications for magmatic processes and source region compositions. *In*: FITTON, J.G., MAHONEY, J.J., WALLACE, P.J. & SAUNDERS, A.D. (eds) *Origin and Evolution of the Ontong Java Plateau*. Geological Society, London, Special Publications, **229**, 239–257.

ROBERGE, J., WALLACE, P.J., WHITE, R.V. & COFFIN, M.F. (2004*b*). Anomalous uplift and subsidence of the Ontong Java Plateau inferred from CO_2 contents of submarine basaltic glasses. Submitted to Geology.

SAUNDERS, A.D., STOREY, M., KENT, R.W. & NORRY, M.J. 1992. Consequences of plume–lithosphere interactions. *In:* STOREY, B.C., ALABASTER, T. & PANKHURST, R.J. (eds) *Magmatism and the Causes of Continental Break Up*. Geological Society, London, Special Publications, **68**, 41–60.

SAUNDERS, A.D., FITTON, J.G., KERR, A.C., NORRY, M.J. & KENT, R.W. 1997. The North Atlantic igneous province. *In*: MAHONEY, J.J. & COFFIN, M.F. (eds) *Large Igneous Provinces: Continental, Oceanic, and Planetary Flood Volcanism*. American Geophysical Union, Geophysical Monograph, **100**, 45–93.

SHAFER, J.T., NEAL, C.R. & CASTILLO, P.R. 2004. Compositional variability in lavas from the Ontong Java Plateau: results from basalt clasts within the volcaniclastic succession at Ocean Drilling Program Site 1184. *In*: FITTON, J.G., MAHONEY, J.J., WALLACE, P.J. & SAUNDERS, A.D. (eds) *Origin and Evolution of the Ontong Java Plateau*. Geological Society, London, Special Publications, **229**, 333–351.

SMITH, W.H.F. & SANDWELL, D.T. 1997. Global seafloor topography from satellite altimetry and ship depth soundings. *Science*, **277**, 1956–1962.

SUN, S.-S. & MCDONOUGH, W.F. 1989. Chemical and isotopic systematics of oceanic basalts: implications for mantle composition and processes. *In*: SAUNDERS, A.D. & NORRY, M.J. (eds) *Magmatism in the Ocean Basins*. Geological Society, London, Special Publications, **42**, 313–345.

TEJADA, M.L.G., MAHONEY, J.J., DUNCAN, R.A. & HAWKINS, M.P. 1996. Age and geochemistry of basement and alkalic rocks of Malaita and Santa Isabel, Solomon Islands, southern margin of Ontong Java Plateau. *Journal of Petrology*, **37**, 361–394.

TEJADA, M.L.G., MAHONEY, J.J., NEAL, C.R., DUNCAN, R.A. & PETTERSON, M.G. 2002. Basement geochemistry and geochronology of Central Malaita, Solomon Islands, with implications for the origin and evolution of the Ontong Java Plateau. *Journal of Petrology*, **43**, 449–484.

TEJADA, M.L.G., MAHONEY, J.J., CASTILLO, P.R., INGLE, S.P., SHETH, H.C. & WEIS, D. 2004. Pin-pricking the elephant: evidence on the origin of the Ontong Java Plateau from Pb–Sr–Hf–Nd isotopic characteristics of ODP Leg 192 basalts. *In*: FITTON, J.G., MAHONEY, J.J., WALLACE, P.J. & SAUNDERS, A.D. (eds) *Origin and Evolution of the Ontong Java Plateau*. Geological Society, London, Special Publications, **229**, 133–150.

THORDARSON, T. 2004. Accretionary-lapilli-bearing pyroclastic rocks at ODP Leg 192 Site 1184A: a record of subaerial phreatomagmatic eruptions on the Ontong Java Plateau. *In*: FITTON, J.G., MAHONEY, J.J., WALLACE, P.J. & SAUNDERS, A.D. (eds) *Origin and Evolution of the Ontong Java Plateau*. Geological Society, London, Special Publications, **229**, 275–306.

TODT, W., CLIFF, R.A., HANZER, A. & HOFMANN, A.W. 1984. $^{202}Pb+^{205}Pb$ double spike for lead isotopic analysis. *Terra Cognita*, **4**, 209.

VERMA, S.P. 1992. Seawater alteration effects on REE, K, Rb, Cs, Sr, U, Th, Pb, and Sr–Nd–Pb isotope systematics of mid-ocean ridge basalt. *Geochemical Journal*, **26**, 159–177.

WHITE, R.V. 1999. *The fundamentals of crust generation: major tonalite intrusions associated with an oceanic plateau, Aruba, Dutch Caribbean*. PhD Thesis, University of Leicester.

WHITE, R.V. 2002. Earth's biggest 'whodunnit': unravelling the clues in the case of the end-Permian mass extinction. *Philosophical Transactions of the Royal Society of London*, **360**, 2963–2985.

WIGNALL, P.B. 2001. Large igneous provinces and mass extinctions. *Earth-Science Reviews*, **53**, 1–33.

YAN, C.Y. & KROENKE, L.W. 1993. A plate tectonic reconstruction of the Southwest Pacific, 100–0 Ma. *In*: BERGER, W.H., KROENKE, L.W., MAYER, L.A. *et al.* (eds) *Proceedings of the Ocean Drilling Program, Scientific Results*, **130**, 697–709.